Human Molecular Genetics, 2009, Vol. 18, No. 20 **3978–3986**
doi:10.1093/hmg/ddp344
Advance Access published on July 24, 2009

Targeted disruption of the *Wnk4* gene decreases phosphorylation of Na-Cl cotransporter, increases Na excretion and lowers blood pressure

Akihito Ohta[1], Tatemitsu Rai[1], Naofumi Yui[1], Motoko Chiga[1], Sung-Sen Yang[2], Shih-Hua Lin[2], Eisei Sohara[1], Sei Sasaki[1] and Shinichi Uchida[1,*]

[1]Department of Nephrology, Graduate School of Medicine, Tokyo Medical and Dental University, Tokyo, Japan and [2]Division of Nephrology, Department of Medicine, Tri-Service General Hospital, Taipei, Taiwan

Received June 15, 2009; Revised July 13, 2009; Accepted July 22, 2009

We recently generated *Wnk4*$^{D561A/+}$ knockin mice and found that a major pathogenesis of pseudohypoaldosteronism type II was the activation of the OSR1/SPAK kinase-NaCl cotransporter (NCC) phosphorylation cascade by the mutant WNK4. However, the physiological roles of wild-type WNK4 on the regulation of Na excretion and blood pressure, and whether wild-type WNK4 functions positively or negatively in this cascade, remained to be determined. In the present study, we generated WNK4 hypomorphic mice by deleting exon 7 of the *Wnk4* gene. These mice did not show hypokalemia and metabolic alkalosis, but they did exhibit low blood pressure and increased Na and K excretion under low-salt diet. Phosphorylation of OSR1/SPAK and NCC was significantly reduced in the mutant mice as compared with their wild-type littermates. Protein levels of ROMK and Maxi K were not changed, but epithelial Na channel appeared to be activated as a compensatory mechanism for the reduced NCC function. Thus, wild-type WNK4 is a positive regulator for the WNK-OSR1/SPAK-NCC cascade, and WNK4 is a potential target of anti-hypertensive drugs.

INTRODUCTION

Pseudohypoaldosteronism type II (PHAII) is an autosomal-dominant disorder characterized by hyperkalemia, metabolic acidosis and hypertension (1–3). In 2001, Wilson *et al*. found that WNK1 and WNK4 gene mutations cause PHAII (4). However, since the physiological function of WNK kinases had not been clarified, the molecular pathogenesis of PHAII was not clear at that time. Since PHAII was known to be caused by dysregulation of NaCl reabsorption and potassium excretion in the kidney (5), many studies have focused on how WNK kinases regulate renal channels and transporters (6–10). Most of these initial studies used the *Xenopus* oocyte expression system (6–10). The Na-Cl cotransporter (NCC) has been postulated as a major target of WNK kinases since PHAII is very sensitive to thiazide diuretics (5). Yang *et al*. (6) and Wilson *et al*. (7) found that wild-type WNK4 inhibited NCC function in the oocyte expression system, but a disease-causing mutant WNK4 lacked this inhibitory effect. On the basis of these data, they speculated that the pathogenesis of PHAII might come from a loss-of-function effect of the mutant. On the other hand, in previous studies with MDCK cells, we found that the inhibitory effect of WNK4 was not specific to NCC but was observed in other transporters not related to PHAII (11). Furthermore, the mutant WNK4 also retained its inhibitory effect in our experiments. Accordingly, as Richardson *et al*. (12,13) recently suggested, we decided to use genetically engineered mice instead of a heterologous overexpression system to clarify the physiological roles of WNK kinases. Recently, mutant WNK4 transgenic mice carrying two additional mutant WNK4 alleles were generated, and they exhibited the PHAII phenotypes (14), clearly indicating that the mutant WNK4 acts as a gain-of-function mutant rather than a loss-of-function mutant. We recently generated *Wnk4*$^{D561A/+}$ knockin mice, an ideal mouse model of PHAII, and found that the major pathogenesis of PHAII *in vivo* is the activation of the phosphorylation cascade of OSR1/SPAK kinase and NCC by the mutant WNK4 (15). Accordingly, the next question was whether the disease-causing mutant WNK4 was

*To whom correspondence should be addressed at: Department of Nephrology, Graduate School of Medicine, Tokyo Medical and Dental University, 1-5-45 Yushima, Bunkyo, Tokyo 113-8519, Japan. Tel: +81 358035214; Fax: +81 358035215; Email: suchida.kid@tmd.ac.jp

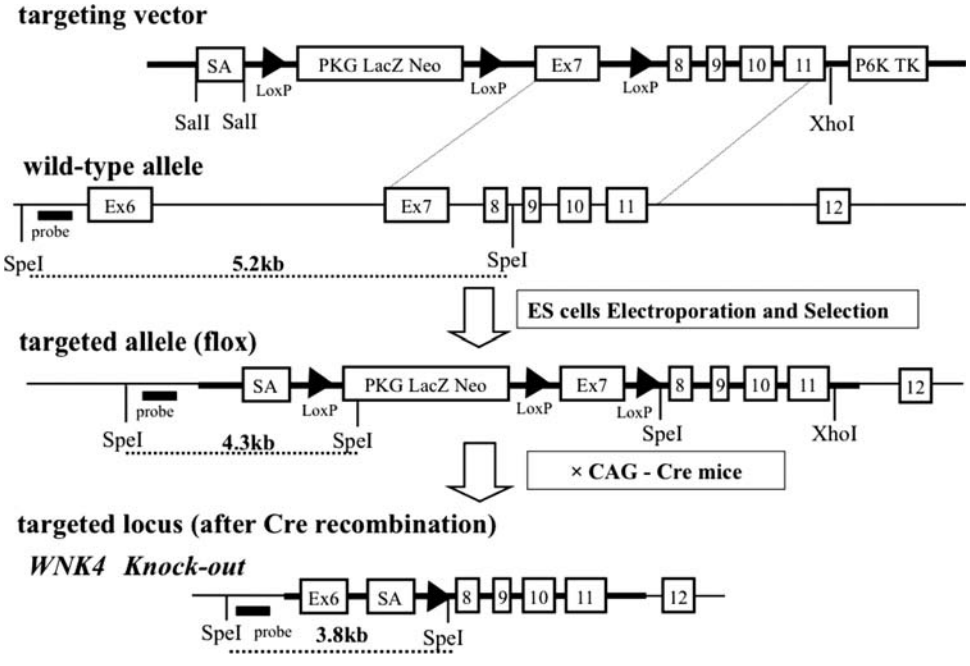

Figure 1. Targeting strategy for generating *Wnk4* hypomorphic mice. This diagram shows the targeting construct, the wild *Wnk4* locus, and the targeted locus before and after Cre recombination. Exon 7 was flanked with two *lox*P sites.

a dominant-active or -negative mutant. In other words, was wild-type WNK4 a positive or negative regulator for this cascade? This simple question has not yet been answered, but it is an important issue for further research on WNK kinases and also a crucial problem when considering the development of anti-hypertensive drugs focusing on WNK kinases. To answer this question, generation and analysis of *Wnk4* null mice is necessary. However, homozygous mice in which the kinase domain of the *Wnk4* gene was targeted showed embryonic lethality (unpublished observation). Therefore, in the present study, we targeted the *Wnk4* gene at different exons and successfully generated WNK4 hypomorphic mice. These mice have lower blood pressure and a reduced NaCl reabsorption capacity as compared with their wild-type littermates, and they also have decreased OSR1/SPAK and NCC phosphorylation.

RESULTS

Characterization of the targeted allele of the *Wnk4* gene

Since we suspected that WNK4 null mice might exhibit embryonic lethality, we planned to generate WNK4 hypomorphic mice. Accordingly, we designed a targeting vector to delete a single exon (exon 7) of the *Wnk4* gene outside the kinase domain (Fig. 1). Homologous recombination was confirmed by PCR and Southern blotting in three ES cell lines, from which the heterozygous mutant mice were successfully generated (Fig. 2A). We observed no phenotypical difference among the three mouse lines. We selected one of the lines for further analyses, and examined the mutant WNK4 mRNA and protein produced in the kidneys of this line. To examine the mRNA, we prepared several primer sets flanking exon 7 and performed RT–PCR. As we expected, the deletion of exon 7 yielded the splicing from exon 6 to 8 (Fig. 2B). In addition, the smaller amount of transcript derived from the splicing from exon 6 to 9 was also detected. No other types of transcripts were detected by RT–PCR with other primer sets. We then used immunoblots to determine if these transcripts were translated into proteins in the kidney. For this purpose, we generated two new antibodies to WNK4 that recognized the amino and carboxy terminal portions of WNK4. The specificity of the antibodies was determined by antigen absorption tests (Supplementary Material, Figure S1). The transcript derived from the splicing from exon 6 to 8 had a frame-shift and should yield a C-terminally truncated WNK4 protein of 63 kD. The transcript derived from the splicing from exon 6 to 9 had no frame-shift, which should result in a ~14 kD smaller protein lacking the middle portion of WNK4 (WNK4ΔEx7-8) than wild-type WNK4. Both antibodies detected a band of the same molecular weight in the mutant mouse kidney. The difference of apparent molecular weight of the bands between the mutant mice and the wild-type littermates were consistent with that estimated from the calculated molecular weight (~14 kD) (Fig. 2C and D). On the basis of these observations, we concluded that the mutant mice expressed the WNK4ΔEx7-8 protein. The C-terminally truncated WNK4 protein was not detected in the mutant mice. The WNK4ΔEx7-8 protein was also detected by immunofluorescence. As shown in Figure 2E, the signal for WNK4ΔEx7-8 was co-localized with the signals for parvalbumin (marker of distal convoluted tubule 1) or calbindin-D28K (marker of distal convoluted tubule 2, connecting tubule and cortical collecting duct), similarly to the signal for wild-type WNK4. Co-localization with parvalbumin plus calbindin-D28K was also confirmed to be similar (data not shown). These results indicate that the intrar-

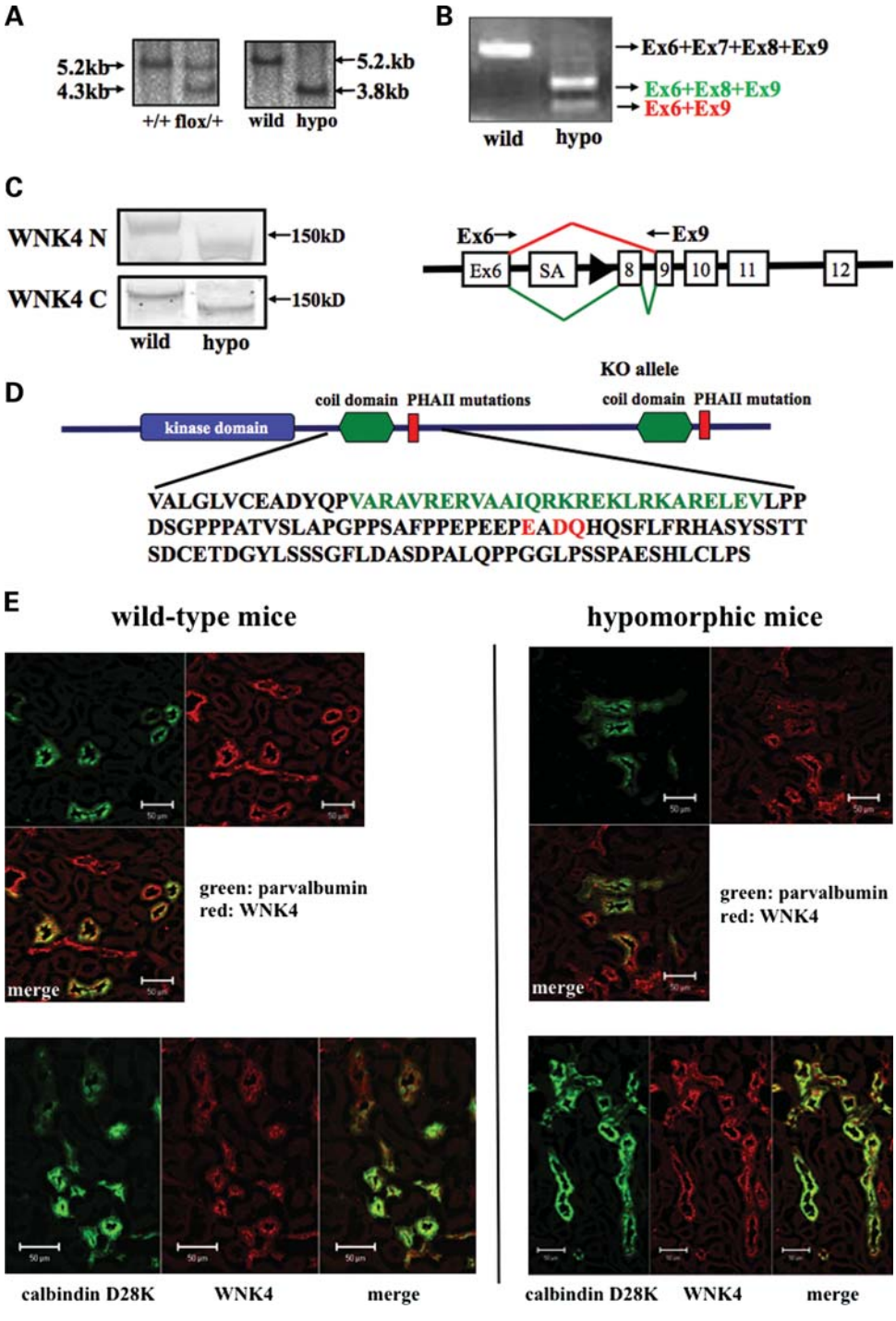

Figure 2. Characterization of the targeted *Wnk4* allele. (**A**) Verification of homologous recombination by Southern blotting. *Spe*I-digested genomic DNA derived from embryonic stems cell clones (left panel) and mouse tails (right panel). The 5.2-kb band is from the wild-type allele, and the 4.3-kb band (left panel) is from the floxed allele. The 3.8-kb band (right panel) is from the mutated allele after Cre recombination. (**B**) RT–PCR products with a primer set designed for exons 6 and 9. Kidney mRNA was isolated from the mutant mice and their wild-type littermates. Sequencing of RT–PCR products revealed that the mutant mouse had two patterns of splicing: the major upper band consisted of the mRNA spliced from exon 6 to 8, and the minor lower band was the transcript consisting of exons 6 and 9. The upper transcript has a shift of the open reading frame in the region corresponding to exon 8, but the open reading frame was preserved after the deletion of the exons 7 and 8 in the lower transcript. (**C**) Immunoblots of WNK4. Two anti-WNK4 antibodies generated against the N-terminus and C-terminal portion of WNK4 were used for immunoblots. Both antibodies detected the same band of WNK4 in the wild-type mice (~155 kD). However, both antibodies recognized a band of lower molecular weight (~140 kD) in the mutant mice. This size difference matched the expected size of WNK4 protein in which exons 7 and 8 were deleted (WNK4ΔEx7-8). (**D**) The amino acid sequence deleted in the WNK4ΔEx7-8. The letters in green indicate a putative coil domain, and the amino acids in red are mutated in PHAII patients. E. Immunofluorescence of WNK4 in the kidney. The anti-WNK4 antibody generated against the N-terminus was used for immunofluorescence. Intrarenal localization of the wild-type WNK4 and WNK4ΔEx7-8 (red) was determined by co-staining with parvalbumin and calbindin-D28K (green), and they did not appear to be different. Bar = 50 μm.

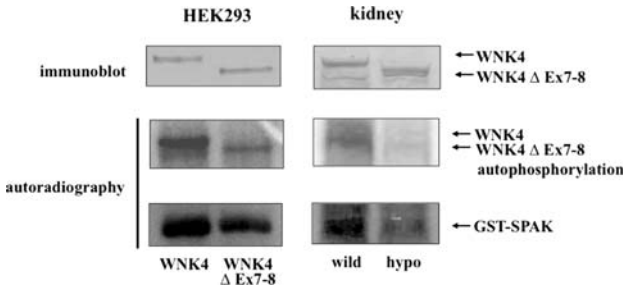

Figure 3. Kinase assay of WNK4ΔEx7-8*in vitro* and *in vivo*. In an *in vitro* assay (left panels), FLAG-tagged WNK4 and FLAG-tagged WNK4 devoid of exons 7 and 8 produced in HEK293 cells by transient transfection were immunoprecipitated with M2-FLAG agarose, incubated with GST-SPAK (17) in a kinase buffer containing γ^{32}P-ATP, separated by SDS-PAGE and visualized by autoradiography. In the *in vivo* assay (right panels), WNK4 and the WNK4ΔEx7-8 protein were immunoprecipitated from the kidney with anti-WNK4 antibody generated against the N-terminus and used for a kinase assay (as described above). Little autophosphorylation of WNK4ΔEx7-8 was observed in the mutant mice, and phosphorylation of GST-SPAK was significantly reduced.

enal localization of WNK4ΔEx7-8 is the same as that of the wild-type WNK4.

Functional characterization of WNK4ΔEx7-8 protein

To determine if the mutant mice constituted a WNK4 hypomorphic model, we characterized the kinase activity of the WNK4ΔEx7-8 protein *in vitro* (HEK293 cell) and *in vivo* (kidney). Both autophosphorylation of WNK4 and phosphorylation of SPAK (the only physiological substrate of WNK4 identified thus far) were greatly reduced by the deletion (Fig. 3), confirming that the mutant mice were indeed WNK4 hypomorphic mice.

Blood and urine analyses

We observed no obvious differences between the WNK4 hypomorphic mice and the wild-type littermates in survival, gross physical appearance and organ morphology. There were no significant differences in the pH, K and HCO3-levels, plasma renin activity and aldosterone levels (Table 1). Hypocalciuria and hypomagnesemia previously observed in the Ncc null mice (16) were also not observed in the WNK4 hypomorphic mice (urine Ca: 0.071 ± 0.007 mg/g Cre in the wild-type mice and 0.073 ± 0.008 mg/g Cre in the hypomorphic mice, $n = 8$; serum Mg: 1.80 ± 0.06 mg/dl in the wild-type mice and 1.72 ± 0.03 mg/dl in the hypomorphic mice, $n = 8$). Urinary excretion of Na and K under normal condition was also not significantly affected in the WNK4 hypomorphic mice (Fig. 4A and B). To more thoroughly characterize the phenotypes, we fed the hypomorphic and wild-type mice low-salt (0.01% NaCl) and high-salt (4% NaCl) diets, and monitored urinary Na and K excretion, particularly focusing on the transition periods in changing diets. As shown in Figure 4A, Na excretion in the hypomorphic mice was significantly higher on days 5, 6 and 7 under the low-salt diets, and during the transitional period from low- to high-salt diet. On days 5, 6 and 7 under low-salt diets, wild-type mice reduced Na excretion to levels estimated to be equivalent to the reduced Na intake. However, the hypomorphic mice could not fully adapt to the reduced NaCl intake. At this phase, both groups of mice were presumably exhibiting their maximum capacity of Na conservation, and the difference in

Table 1. Blood data

	Wild-type mice ($n = 8$)	Hypomorphic mice ($n = 7$)
Na (mmol/l)	149.1 ± 0.6	148.7 ± 0.5
K (mmol/l)	4.3 ± 0.1	4.1 ± 0.1
Cl (mmol/l)	114.1 ± 0.5	114.1 ± 0.7
$HCO3^-$ (mmol/l)	21.6 ± 0.7	21.5 ± 0.7
Cre (mg/dl)	0.222 ± 0.014	0.214 ± 0.014
pH (venous)	7.28 ± 0.02	7.24 ± 0.01
PRA (ng/ml/h)	23.8 ± 2.6	21.5 ± 4.1
Aldosterone (pg/ml)	358.5 ± 30.2	427.4 ± 69.3

Values in mean ± SEM.

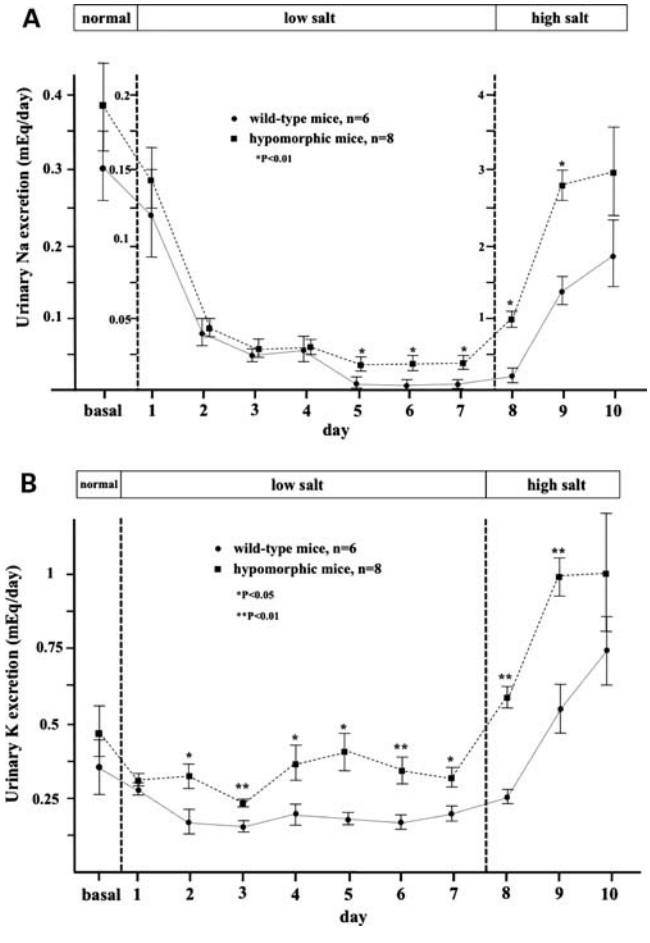

Figure 4. Excretion of Na and K under low and high salt diets. (**A**) Na excretion in hypomorphic mice (closed squares, $n = 8$, mean ± SEM) and their littermates (closed circles, $n = 6$, mean ± SEM) under low- (0.01% NaCl) and high-salt diets (4% NaCl). Data under normal diet (0.4% NaCl) was the mean of data on three consecutive days. On day 0, mice were switched from normal diet to low-salt diet, and on day 7, they were switched to high-salt diet. Note that the scale of the *y*-axis under each diet is different. There were significant differences ($^*P < 0.01$) in Na excretion between the groups. (**B**) K excretion in hypomorphic mice (closed squares, $n = 8$) and their littermates (closed circles, $n = 6$) under low- and high-salt diets. $^*P < 0.05$, $^{**}P < 0.01$.

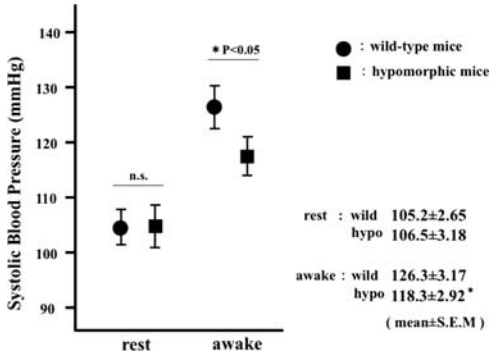

Figure 5. Telemetric measurement of blood pressure. Systolic blood pressure of the hypomorphic mice during their active period was significantly lower than that in their wild-type littermates ($P < 0.05$).

this capacity was also evident when the mice were abruptly switched to high-salt diet. Although we could not detect any differences in the serum K levels between wild-type and hypomorphic mice, even under low-K diet (serum K: 2.94 ± 0.14 mEq/l in wild-type mice and 3.20 ± 0.20 mEq/l in hypomorphic mice, $n = 8$), increased K excretion was also detected in hypomorphic mice in the metabolic cage study (Fig. 4B).

Blood pressure

We used radiotelemetric devices to measure blood pressure under physiological conditions. As shown in Figure 5, although no significant difference in blood pressure was detected in the resting period (day time) between the two groups, the systolic blood pressure of the hypomorphic mice was significantly lower than that of their wild-type littermates during the period of high-activity (118.3 ± 2.92 versus 126.3 ± 3.17 mmHg, $n = 6$, $P < 0.05$). Under low-salt diet, the results were almost the same as those under normal diet (day: 106 ± 2.01 versus 109 ± 0.64 mmHg, no significant difference; night: 119 ± 1.43 versus 133 ± 2.19 mmHg, $n = 3$, $P < 0.05$). Further decreases in blood pressure under low-salt diet were not observed in either wild-type or hypomorphic mice.

Reduced phosphorylation of OSR1 and NCC in the WNK4 hypomorphic mice

We investigated the phosphorylation status of the downstream targets of WNK4. As expected from the *in vivo* kinase assay (Fig. 3), phosphorylation level of OSR1 at the specific site phosphorylated by WNK kinase were significantly decreased in the WNK4 hypomorphic mice as compared with their wild-type littermates (Fig. 5A). Phosphorylations of NCC at T53, T58 and S71 were also dramatically reduced in the hypomorphic WNK4 mice, although the total amount of NCC was unchanged (Fig. 5B). Since *in vitro* studies reported that kidney K and Na channels were regulated by WNK4, we also investigated the protein levels of these channels by immunoblots. Protein levels of ROMK and maxi-K were not changed in the hypomorphic mice (Fig. 6A). As for the epithelial Na channel (ENaC), alpha-, beta- and gamma-ENaC

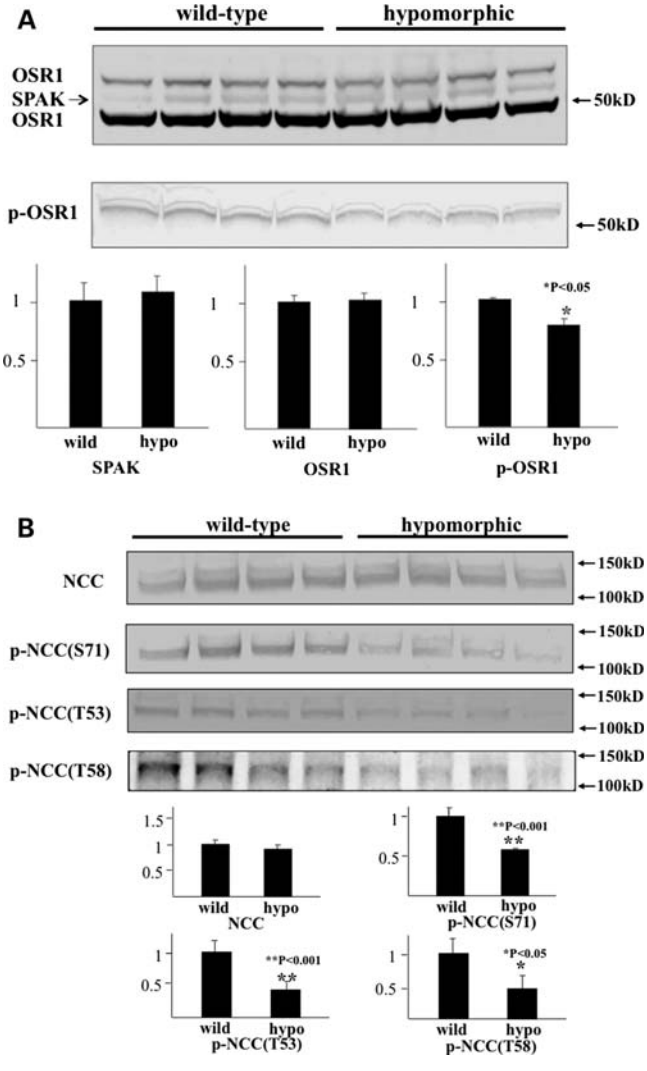

Figure 6. Phosphorylation status of OSR1 and NCC. (**A**) Although the amounts of total OSR1 and SPAK were not changed in the hypomorphic mice, the phosphorylated OSR1 was significantly decreased ($*P < 0.05$) in the hypomorphic mice. (**B**) The amounts of phosphorylated NCC at three sites (T53, T58, S71) were significantly reduced in the hypomorphic mice without an apparent change in the total NCC content.

plus cleaved alpha- and gamma-ENaC were significantly increased in the hypomorphic mice (Fig. 6B).

DISCUSSION

In this study, we successfully generated and analyzed WNK4 hypomorphic mice. The expression of WNK4ΔEx7-8 protein in the mutant mice prevented the embryonic lethality observed in total WNK4 knockout mice. We performed *in vitro* and *in vivo* kinase assays that demonstrated the decreased kinase activity of WNK4ΔEx7-8 protein. Furthermore, the phenotypes were only observed in the homozygous mice, not in the heterozygous mice (data not shown), indicating that the phenotypes are caused by the reduced activity of WNK4, not by some unexpected dominant-negative functions of the mutant WNK4 on other WNK kinases or OSR1/SPAK.

Therefore, we regard the mutant mice as WNK4 hypomorphic mice. The generation of this mutant enabled us to investigate *in vivo* the consequence of reduced WNK4 activity in the kidney function.

The hypomorphic mice did not show the typical phenotypes (hypokalemia, alkalosis, hypomagnesemia and increased renin activity and aldosterone) of human Gitelman syndrome under normal diet. However, even the Ncc-null mice did not completely mimic the physiological findings observed in Gitelman's patients (16). As the NCC protein was conserved and NCC phosphorylation was not completely absent in hypomorphic mice, the phenotypes were expected to be milder than those in Ncc-null mice. Nonetheless, we detected clear reductions in peak ability to conserve Na under Na-deprived and subsequent Na-loaded conditions (Fig. 4A). The difference in K excretion between hypomorphic and wild-type mice was more evident than that in Na excretion (Fig. 4B) on day 2, thus suggesting that the decreased function of NCC by in WNK4 hypomorphic mice increases Na delivery to the downstream nephron segment where Na/K exchange occurs. In addition, the lower blood pressure and decreased OSR1 and NCC phosphorylation in WNK4 hypomorphic mice (Figs 5 and 6) clearly demonstrate that WNK4 positively regulates NCC function *in vivo* through the OSR1/SPAK-NCC phosphorylation cascade.

The study of *Wnk4*^{D561A} knockin mice suggested that WNK-OSR1/SPAK-NCC constitutes a kinase cascade in *in vivo* kidney. However, whether WNK4(D561A) was acting as a dominant-active or -negative mutant in this cascade could not be determined, since the role of wild-type WNK4 in this cascade was not clarified. Our *in vitro* phosphorylation study (17) showed that WNK4 as well as WNK1 phosphorylates their substrates, OSR1 and SPAK kinases, suggesting that wild-type WNK4 sends a positive signal at least to OSR1/SPAK. Accordingly, it may be reasonable to speculate that wild-type WNK4 is a positive regulator of NCC. In the present study, we demonstrate that a reduction of WNK4 kinase activity *in vivo* leads to reduced NCC phosphorylation, lower blood pressure and reduced capacity of NaCl reabsorption. We previously showed that phosphorylation was important for the localization of NCC on the apical plasma membranes in the distal convoluted tubules, and Pacheco-Alvarez *et al*. (18) reported that phosphorylation itself was necessary for the functional activation of NCC. Whether the regulation of NCC by phosphorylation is a functional activation of the transporter itself or is mediated by intracellular sorting mechanisms or both, both data clearly indicates that the phosphorylation of NCC up-regulates its function *in vivo*. In this respect, we can conclude that wild-type WNK4 is a positive regulator for NCC at least through the WNK-OSR1/SPAK-NCC cascade. In contrast, other studies have suggested that wild-type WNK4 is a negative regulator for NCC. However, such data on NCC regulation by WNK kinases relied on overexpression systems including *Xenopus* oocytes (6,7) and transgenic mice (14), and the scheme of NCC regulation by WNK kinases was depicted in the absence of OSR1/SPAK kinases and phosphorylation of NCC [see reviews by McCormick (19) and Richardson (12)]. Wilson *et al*. (7) reported that the inhibitory effect of wild-type WNK4 on NCC was dependent on WNK4 kinase activity. On the other hand, Yang *et al*. (6) showed that it was not kinase-dependent, instead it was mediated by the carboxy terminal portion of WNK4. If it is a kinase-dependent process, NCC must be up-regulated in the WNK4 hypomorphic mice since the mice had reduced WNK4 kinase activity. However, the phenotypes that we observed do not match this hypothesis, suggesting that the inhibitory function of WNK4 observed in oocytes occurs only minimally *in vivo*. However, if the inhibitory effect observed in oocytes is not dependent on WNK4 kinase activity, we must wait until conditional WNK4 null mice are generated to answer this question, since the carboxy terminal portion of WNK4 remains in the WNK4 hypomorphic mice. This situation is similar to determining if ENaC is a direct target of WNK4, since Ring *et al*. (9) reported that wild-type WNK4 inhibited ENaC activity in oocytes in a manner that was not kinase activity-dependent. However, we believe that the up-regulation of ENaC observed in the hypomorphic mice is not a primary effect of the WNK4 hypomorph; rather, it is a compensatory mechanism for the reduction of NCC function as long as the phenotypes in the hypomorphic mice are not hypertension but low blood pressure and NaCl-losing. Accordingly, we think that the activation of ENaC provides evidence that NCC function is indeed decreased *in vivo*.

Although the issue of whether WNK4 is a positive or negative regulator of NCC was settled, as described above, there are some unresolved issues regarding the phenotypes of hypomorphic mice. Increased K excretion was still observed after Na excretion reached a steady state under the low-salt diet (days 5–7). Even if we consider ENaC activation in the hypomorphic mice, the difference in Na excretion may not have been sufficient to account for the differences in K excretion by Na/K exchange alone. This suggests that K excretion mechanism(s) other than Na/K exchange are increased directly or indirectly in WNK4 hypomorphic mice. With regard to the lower blood pressure in the hypomorphic mice, we were unable to observe further decreases with a low-salt diet. Thus, our observation period may not have been sufficiently long (up to 10 days under low-salt diet) to detect the difference.

WNK kinases have been thought to be target molecules for anti-hypertensive drugs since the discovery of mutations in the WNK kinases in PHAII. However, the kinase domains of WNK kinases (WNK1-4) are highly similar, making it difficult to develop isoform-specific inhibitors. If the effect of each WNK on NCC is variable (20,21) (i.e. WNK4 is inhibitory and WNK3 is stimulatory), inhibitors to WNK kinases may not be promising as anti-hypertensive drugs. In this respect, the present study, along with the study of the *Wnk1*$^{+/-}$ mice (22), tells us that the inhibition of WNK kinases may be beneficial for reducing blood pressure.

In conclusion, the generation and analyses of the WNK4 hypomorphic mice clarified that WNK4 kinase activity is important for maintaining NCC function by phosphorylation.

MATERIALS AND METHODS

Targeted disruption of the *Wnk4* gene

To perform targeted disruption of the *Wnk4* gene, we prepared the targeting vector by using PCR-amplified segments of the

Wnk4 gene after verifying the sequences (Fig. 1). The targeting vector was then transfected into J1 ES cells by electroporation, as described previously (23). After selection with 150 μg/ml G418 and 2 μM ganciclovir, targeted embryonic stem cell clones were selected by PCR and Southern blotting. Chimeric male mice were bred with C57BL/6 females to produce the heterozygous floxed mice, and the neo cassette was then deleted by crossing the mice with Cre recombinase-expressing transgenic mice (24). This experiment was approved by the Animal Care and Use Committee of Tokyo Medical and Dental University.

Blood pressure measurements

We measured blood pressure by a radiotelemetric method (25) in which a blood pressure transducer (Data Sciences International, St Paul, MN, USA) was inserted into the left carotid artery. Ten days after transplantation, each mouse was housed individually in a standard cage on a receiver under a 12-h light-dark cycle. Systolic and diastolic blood pressure, heart rate and activity were recorded every minute by radiotelemetry. Mice showed alternating periods of high-activity (10 p.m.–4 a.m.) and low-activity (10 a.m–4 p.m.), as reported previously (26). For each mouse, we measured blood pressure values for more than three consecutive days and calculated the mean ± SEM of all values during both high- and low-activity periods.

Blood and urine measurements

Blood for electrolyte analyses was obtained from the retro-orbital sinus under light ether anesthesia. Electrolyte levels were determined with an i-STAT analyzer (Fuso, Osaka, Japan). The serum aldosterone level and plasma renin activity were measured by the SRL Clinical Laboratory Service (Tokyo, Japan). Low-salt (0.01% NaCl), high-salt (4% NaCl) and low-potassium (0.03%) diets were obtained from Oriental Yeast Co., Ltd (Tokyo, Japan). Urine samples were analyzed by DRI-CHEM (Fujifilm, Tokyo, Japan).

Immunoblotting and immunofluorescence

Semiquantitative immunoblotting was performed as described previously (15) by using whole kidney homogenate without the nuclear fraction (600*g*) or the crude membrane fraction (17 000*g*). The intensity of bands was analyzed by using Image-Gauge software (Fujifilm). For immunofluorescence staining, kidneys were fixed by perfusion through the left ventricle with periodate lysine (0.2 M) and paraformaldehyde (2%) in PBS. Tissue samples were soaked for several hours in 20% sucrose in PBS, embedded in Tissue-Tek OCT Compound (Sakura Finetechnical Co., Ltd, Tokyo, Japan), and snap frozen in liquid nitrogen. We generated two anti-WNK4 antibodies, recognizing the N-terminus (MLAPRNTETGVPMS) and the C-terminal portion (QRSDNLPGPGIMRRN) of mouse WNK4. The specificity of these anti-WNK4 antibodies was verified by antigen absorption tests (Supplementary Material, Figure S1). The antibody recognizing the N-terminus of WNK4 was better than the C-terminal antibody at detecting WNK4 in immunofluorescence assays (Supplementary Material, Figure S2). After we used our entire initial batch of anti-OSR1/SPAK and anti-phosphorylated OSR1/SPAK antibodies, we produced a second batch with the same antigen peptides (17). The initial batches recognized multiple bands around 70 kD in addition to bands around 50 kD (15). We tentatively labeled the bands around 70 and 50 kD as SPAK and OSR1, respectively, on the basis of the previous study (27). In this study, we re-evaluated the specificity of several OSR1/SPAK antibodies, including our own, using T7-tagged OSR1 and SPAK as controls. As shown in Supplementary Material, Figure S3, the new batch of anti-total OSR1/SPAK antibody recognized both OSR1 and SPAK, but the sensitivity was slightly better for OSR1 than for SPAK. The major band detected by this antibody in mouse kidney was identified as OSR1 by comparing the results obtained by OSR1-specific (M09; Abnova, Taipei, Taiwan) and SPAK-specific (Cell Signaling Technology, Danvers, MA, USA) antibodies. With regard to anti-phosphosrylated-OSR1/SPAK antibody, the new batch scarcely detected p-SPAK, as shown in Supplementary Material, Figure S4. Accordingly, the band we detected in the kidney samples were regarded as p-OSR. As in the case with

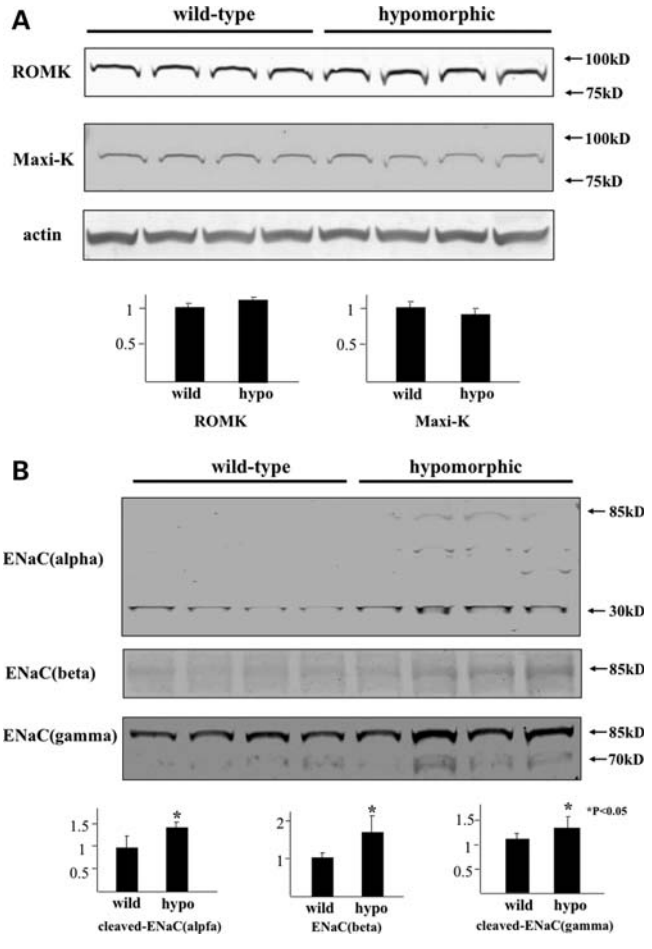

Figure 7. Immunoblots of ROMK1, Maxi-K and ENaC channels. (**A**) No differences in the amount of potassium channels were seen between the hypomorphic mice and their wild-type littermates. (**B**) The protein expression of full-length ENaCs (α, β, and γ at ∼85 kD) and cleaved-ENaCs (α at 30 kD and γat 70 kD) was increased in the hypomorphic mice. Equal loading of protein in each lane was verified by β-actin immunoblot shown in A.

of anti-total OSR1/SPAK antibody, the previous batch of anti-p-OSR1/SPAK appeared to have a better sensitivity to p-SPAK than the new batch. The following primary antibodies were also used in this study: rabbit anti-NCC (1 : 200) (Chemicon, Billerica, MA, USA); rabbit anti-ROMK1 (1 : 200), rabbit anti-maxi K (1 : 100) and rabbit anti-ENaCβ (1 : 200) (Alomone, Israel); rabbit anti-ENaCα, ENaCβ and ENaCγ (1 : 200) (kindly provided by M. Knepper from the NIH, Bethesda, MA, USA); and mouse anti-calbindin-D28K and anti-parvalbumin (1 : 10 000) (Swant, Bellinzona, Switzerland). Alkaline-phosphatase-conjugated anti-IgG antibodies (Promega, Madison, WI, USA) were used as secondary antibodies for immunoblotting, and Alexa 488- or 546-conjugated secondary antibodies were used for immunofluorescense. Immunofluorescense images were obtained by LSM510 Meta (Carl Zeiss, Oberkochen, Germany) (Fig. 7).

Kinase assays

Expression vectors (pTRE2-hyg) of FLAG-tagged whole WNK4 and WNK4 lacking exons 7 and 8 were prepared by PCR. HEK293 cells were transfected with the expression vectors with lipofectamine. Twenty-four hours after transfection, cells were lysed in a lysis-buffer (150 mM NaCl, 15 mM Tris, 1% Triton-X100 and protease inhibitors), and FLAG-tagged WNK4 proteins were immunoprecipitated with M2-agarose (Sigma) for 2 h at 4°C. Then, the immunoprecipitated wild-type and mutant WNK4 proteins were incubated with GST-SPAK in a kinase buffer [50 mM Tris–HCl, ph 7.5, 10 mM $MgCl_2$ and 100 μM(γ^{32P})ATP (2 μCi)] for 20 min at 30°C. The reaction was terminated by adding SDS sample-buffer and boiling for 5 min. Autophosphorylation of WNK4 and phosphorylation of GST-SPAK were visualized by autoradiography, and the bands were analyzed with an image analyzer (Fuji BAS, Tokyo, Japan). For *in vivo* kinase assays, the endogenous WNK4 proteins from the kidney tissue of wild-type and mutant mice were immunoprecipitated with anti-WNK4 antibody recognizing the N-terminus of mouse WNK4.

Statistical methods

Statistical significance was evaluated by un-paired *t*-test. *P*-values <0.05 were considered statistically significant.

SUPPLEMENTARY MATERIAL

Supplementary Material is available at *HMG* online.

Conflict of Interest statement. None declared.

FUNDING

This study was supported in part by Grants-in-Aid for Scientific Research on Priority Areas from the Ministry of Education, Culture, Sports, Science and Technology of Japan, Grants-in-Aid for Scientific Research on Creative Scientific Research from the Japan Society for the Promotion of Science, Japan-Taiwan Joint Research Program for Interchange Association Japan and the Salt Science Research Foundation (#0832).

REFERENCES

1. Gordon, R.D. (1986) Syndrome of hypertension and hyperkalemia with normal glomerular filtration rate. *Hypertension*, **8**, 93–102.
2. Schambelan, M., Sebastian, A. and Rector, F.C. Jr (1981) Mineralocorticoid-resistant renal hyperkalemia without salt wasting (type II pseudohypoaldosteronism): role of increased renal chloride reabsorption. *Kidney Int.*, **19**, 716–727.
3. Achard, J.M., Disse-Nicodeme, S., Fiquet-Kempf, B. and Jeunemaitre, X. (2001) Phenotypic and genetic heterogeneity of familial hyperkalaemic hypertension (Gordon syndrome). *Clin. Exp. Pharmacol. Physiol.*, **28**, 1048–1052.
4. Wilson, F.H., Disse-Nicodeme, S., Choate, K.A., Ishikawa, K., Nelson-Williams, C., Desitter, I., Gunel, M., Milford, D.V., Lipkin, G.W., Achard, J.M. *et al.* (2001) Human hypertension caused by mutations in WNK kinases. *Science*, **293**, 1107–1112.
5. Mayan, H., Vered, I., Mouallem, M., Tzadok-Witkon, M., Pauzner, R. and Farfel, Z. (2002) Pseudohypoaldosteronism type II: marked sensitivity to thiazides, hypercalciuria, normomagnesemia, and low bone mineral density. *J. Clin. Endocrinol. Metab.*, **87**, 3248–3254.
6. Yang, C.L., Angell, J., Mitchell, R. and Ellison, D.H. (2003) WNK kinases regulate thiazide-sensitive Na-Cl cotransport. *J. Clin. Invest.*, **111**, 1039–1045.
7. Wilson, F.H., Kahle, K.T., Sabath, E., Lalioti, M.D., Rapson, A.K., Hoover, R.S., Hebert, S.C., Gamba, G. and Lifton, R.P. (2003) Molecular pathogenesis of inherited hypertension with hyperkalemia: the Na-Cl cotransporter is inhibited by wild-type but not mutant WNK4. *Proc. Natl. Acad. Sci. U.S.A.*, **100**, 680–684.
8. Kahle, K.T., Gimenez, I., Hassan, H., Wilson, F.H., Wong, R.D., Forbush, B., Aronson, P.S. and Lifton, R.P. (2004) WNK4 regulates apical and basolateral Cl- flux in extrarenal epithelia. *Proc. Natl. Acad. Sci. U.S.A.*, **101**, 2064–2069.
9. Ring, A.M., Cheng, S.X., Leng, Q., Kahle, K.T., Rinehart, J., Lalioti, M.D., Volkman, H.M., Wilson, F.H., Hebert, S.C. and Lifton, R.P. (2007) WNK4 regulates activity of the epithelial Na+ channel *in vitro* and *in vivo*. *Proc. Natl. Acad. Sci. U.S.A.*, **104**, 4020–4024.
10. Kahle, K.T., Wilson, F.H., Leng, Q., Lalioti, M.D., O'Connell, A.D., Dong, K., Rapson, A.K., MacGregor, G.G., Giebisch, G., Hebert, S.C. *et al.* (2003) WNK4 regulates the balance between renal NaCl reabsorption and K+ secretion. *Nat. Genet.*, **35**, 372–376.
11. Yang, S.S., Yamauchi, K., Rai, T., Hiyama, A., Sohara, E., Suzuki, T., Itoh, T., Suda, S., Sasaki, S. and Uchida, S. (2005) Regulation of apical localization of the thiazide-sensitive NaCl cotransporter by WNK4 in polarized epithelial cells. *Biochem. Biophys. Res. Commun.*, **330**, 410–414.
12. Richardson, C. and Alessi, D.R. (2008) The regulation of salt transport and blood pressure by the WNK-SPAK/OSR1 signalling pathway. *J. Cell. Sci.*, **121**, 3293–3304.
13. Richardson, C., Rafiqi, F.H., Karlsson, H.K., Moleleki, N., Vandewalle, A., Campbell, D.G., Morrice, N.A. and Alessi, D.R. (2008) Activation of the thiazide-sensitive Na+-Cl- cotransporter by the WNK-regulated kinases SPAK and OSR1. *J. Cell. Sci.*, **121**, 675–684.
14. Lalioti, M.D., Zhang, J., Volkman, H.M., Kahle, K.T., Hoffmann, K.E., Toka, H.R., Nelson-Williams, C., Ellison, D.H., Flavell, R., Booth, C.J. *et al.* (2006) Wnk4 controls blood pressure and potassium homeostasis via regulation of mass and activity of the distal convoluted tubule. *Nat. Genet.*, **38**, 1124–1132.
15. Yang, S.S., Morimoto, T., Rai, T., Chiga, M., Sohara, E., Ohno, M., Uchida, K., Lin, S.H., Moriguchi, T., Shibuya, H. *et al.* (2007) Molecular pathogenesis of pseudohypoaldosteronism type II: generation and analysis of a Wnk4(D561A/+) knockin mouse model. *Cell Metab.*, **5**, 331–344.
16. Schultheis, P.J., Lorenz, J.N., Meneton, P., Nieman, M.L., Riddle, T.M., Flagella, M., Duffy, J.J., Doetschman, T., Miller, M.L. and Shull, G.E. (1998) Phenotype resembling Gitelman's syndrome in mice lacking the apical Na+-Cl- cotransporter of the distal convoluted tubule. *J. Biol. Chem.*, **273**, 29150–29155.
17. Moriguchi, T., Urushiyama, S., Hisamoto, N., Iemura, S., Uchida, S., Natsume, T., Matsumoto, K. and Shibuya, H. (2005) WNK1 regulates phosphorylation of cation-chloride-coupled cotransporters via the

STE20-related kinases, SPAK and OSR1. *J. Biol. Chem.*, **280**, 42685–42693.
18. Pacheco-Alvarez, D., Cristobal, P.S., Meade, P., Moreno, E., Vazquez, N., Munoz, E., Diaz, A., Juarez, M.E., Gimenez, I. and Gamba, G. (2006) The Na+:Cl- cotransporter is activated and phosphorylated at the amino-terminal domain upon intracellular chloride depletion. *J. Biol. Chem.*, **281**, 28755–28763.
19. McCormick, J.A., Yang, C.L. and Ellison, D.H. (2008) WNK kinases and renal sodium transport in health and disease: an integrated view. *Hypertension*, **51**, 588–596.
20. Rinehart, J., Kahle, K.T., de Los Heros, P., Vazquez, N., Meade, P., Wilson, F.H., Hebert, S.C., Gimenez, I., Gamba, G. and Lifton, R.P. (2005) WNK3 kinase is a positive regulator of NKCC2 and NCC, renal cation-Cl- cotransporters required for normal blood pressure homeostasis. *Proc. Natl. Acad. Sci. U.S.A.*, **102**, 16777–16782.
21. Yang, C.L., Zhu, X. and Ellison, D.H. (2007) The thiazide-sensitive Na-Cl cotransporter is regulated by a WNK kinase signaling complex. *J. Clin. Invest.*, **117**, 3403–3411.
22. Zambrowicz, B.P., Abuin, A., Ramirez-Solis, R., Richter, L.J., Piggott, J., BeltrandelRio, H., Buxton, E.C., Edwards, J., Finch, R.A., Friddle, C.J. *et al.* (2003) Wnk1 kinase deficiency lowers blood pressure in mice: a gene-trap screen to identify potential targets for therapeutic intervention. *Proc. Natl. Acad. Sci. U.S.A.*, **100**, 14109–14114.
23. Sohara, E., Rai, T., Yang, S.S., Uchida, K., Nitta, K., Horita, S., Ohno, M., Harada, A., Sasaki, S. and Uchida, S. (2006) Pathogenesis and treatment of autosomal-dominant nephrogenic diabetes insipidus caused by an aquaporin 2 mutation. *Proc. Natl. Acad. Sci. U.S.A.*, **103**, 14217–14222.
24. Sakai, K. and Miyazaki, J. (1997) A transgenic mouse line that retains Cre recombinase activity in mature oocytes irrespective of the cre transgene transmission. *Biochem. Biophys. Res. Commun.*, **237**, 318–324.
25. Mills, P.A., Huetteman, D.A., Brockway, B.P., Zwiers, L.M., Gelsema, A.J., Schwartz, R.S. and Kramer, K. (2000) A new method for measurement of blood pressure, heart rate, and activity in the mouse by radiotelemetry. *J. Appl. Physiol.*, **88**, 1537–1544.
26. Whitesall, S.E., Hoff, J.B., Vollmer, A.P. and D'Alecy, L.G. (2004) Comparison of simultaneous measurement of mouse systolic arterial blood pressure by radiotelemetry and tail-cuff methods. *Am. J. Physiol. Heart Circ. Physiol.*, **286**, H2408–H2415.
27. Gagnon, K.B., England, R. and Delpire, E. (2006) Characterization of SPAK and OSR1, regulatory kinases of the Na-K-2Cl cotransporter. *Mol. Cell. Biol.*, **26**, 689–698.